Journal of Histochemistry & Cytochemistry 2020, Vol. 68(1) 75–91

DOI: 10.1369/0022155419884879
journals.sagepub.com/home/jhc
SAGE

Tissue-specific Fixation Methods Are Required for Optimal In Situ Visualization of Hyaluronan in the Ovary, Kidney, and Liver

Jennifer E. Rowley*, Gillian E. Rubenstein*†, Sharrón L. Manuel, Natalie L. Johnson, Jordan Surgnier, Pinelopi P. Kapitsinou, Francesca E. Duncan,† and Michele T. Pritchard

Department of Obstetrics and Gynecology, Feinberg School of Medicine, Northwestern University, Chicago, Illinois (JER, GER, SLM, FED) and Department of Pharmacology, Toxicology and Therapeutics (NLJ, JS, MTP), Liver Center (MTP), and Department of Internal Medicine, Division of Nephrology and Hypertension (PPK), University of Kansas Medical Center, Kansas City, Kansas

Summary

Hyaluronan (HA) is a ubiquitous component of the extracellular matrix. The spatial-temporal localization of HA can be visualized in situ using biotinylated HA binding proteins (HABPs). This assay is sensitive to fixation conditions, and there are currently no best practices for HA detection. Thus, the goal of this study was to optimize fixation conditions for visualizing HA in the ovary, kidney, and liver through analysis of six commonly used fixatives for HA detection: Bouin's Solution, Carnoy's Solution, Ethanol-Formalin-Glacial Acetic Acid (EFG), Histochoice, Modified Davidson's Solution, and 10% Neutral Buffered Formalin. Organs were harvested from CB6F1 mice and fixed with one of the identified fixatives. Fixed organs were sectioned, and the HABP assay was performed on sections in parallel. Hematoxylin and eosin staining was also performed to visualize tissue architecture. HABP signal localization and intensity varied between fixatives. EFG and Carnoy's Solution best preserved the HA signal intensity in the ovary and liver, showing HA localization in various sub-organ structures. In the kidney, only Modified Davidson's Solution was less than optimal. Our findings demonstrate that fixation can alter the ability to detect HA in tissue macro- and microstructures, as well as localization in a tissue-specific manner, in situ. (J Histochem Cytochem 68:75–91, 2020)

Keywords

extracellular matrix, hyaluronan binding protein assay, preservation—biological, staining/labeling

Introduction

Hyaluronan (HA) is a ubiquitous component of the extracellular matrix (ECM) in vertebrate tissues.[1,2] HA is an unbranched, non-sulfated glycosaminoglycan consisting of repeating glucuronic acid and *N*-acetylglucosamine units, and has numerous distinct biological functions. Through associations with other ECM components, such as proteoglycans, HA provides structural organization and integrity to the ECM.[3] At physiological pH, HA is highly anionic and thus hydrophilic. As a result, HA can bind to water up to 1000-fold its own weight. Thus, HA is critical for

Received for publication May 30, 2019; accepted September 30, 2019.

*These authors contributed equally to this work.
†Member of The Histochemical Society at the time of publication.

Corresponding Authors:
Francesca E. Duncan, Department of Obstetrics and Gynecology, Feinberg School of Medicine, Northwestern University, 303 E. Superior Street, Lurie 7-117, Chicago, IL 60611, USA.
E-mail: f-duncan@northwestern.edu

Michele T. Pritchard, Department of Pharmacology, Toxicology and Therapeutics, University of Kansas Medical Center, 3901 Rainbow Blvd., MS-1018, Kansas City, KS 66160, USA.
E-mail: mpritchard@kumc.edu

Journal of Histochemistry & Cytochemistry

hydration and lubrication in tissues, particularly soft connective tissues and joints.[4] In addition to its structural role, HA is also a potent signaling molecule and mediates cell motility, adhesion, and proliferation.[5–7]

HA abundance and distribution in vivo is dynamic, with particularly striking differences between homeostatic and pathologic conditions. Under homeostatic conditions, HA levels are tightly regulated by a network of enzymes. HA synthases (HAS) produce HA polymers and extrude HA into the extracellular matrix,[8,9] whereas hyaluronidases fragment and degrade HA.[10] HA can also undergo fragmentation in the presence of reactive oxygen species.[11,12] Homeostatic HA levels and distribution are largely maintained in healthy tissues. However, in response to tissue injury or insult, expression and activity of HA-synthesizing and degrading enzymes can become dysregulated, resulting in changes in total HA levels and fragment accumulation, which in turn stimulate inflammatory responses.[13–17] HA levels can increase or decrease at the onset of several disease processes.[18,19] For example, HA levels are elevated in several cancers, including breast, prostate, lung, ovary, bladder, pancreas, and colon.[20–26] In addition, HA levels in bronchoalveolar lavage fluid are significantly increased in asthma patients and are highly correlated with asthma severity.[27–29]

Despite its biological importance, studying tissue HA levels and localization is challenging because this molecule is non-immunogenic. Therefore, examining HA using robust antibody-based approaches is not possible. Several methods, however, have been developed to assess HA content in biological fluids and in tissues, though many of these methods detect relative amounts of different glycosaminoglycans.[30] The most specific methods are enzyme-linked sorbent assays (ELSAs) that use HA-binding proteins (HABPs) that bind to HA but not to other glycosaminoglycans.[31,32] However, these assays are performed on biological samples containing HA, and do not provide insight into the spatial-temporal localization or accumulation of HA in situ. To overcome this limitation, the HABP assay was developed.[33] This assay utilizes a highly specific HABP comprised of either the G1 HA-binding domain of aggrecan or the G1 domain combined with the "link" protein of cartilage to stabilize G1 binding to HA which act as an HA-specific probe.[34] These proteins are typically isolated from bovine nasal cartilage. After isolation, HABP is biotinylated and applied to fixed biological samples (either cells or histological samples) to bind to endogenous HA. Next, avidin, which binds to biotin with high affinity, is applied to the sample. Several studies have successfully used fluorophore- or enzyme-conjugated streptavidin, which allows for the direct detection of the biotinylated-HABP.[35,36] We have expanded on this system to include a tyramide signal amplification step, where fluorescein is deposited in the area where avidin–biotin complexes are bound to HABP, which enhances fluorescent signal.[37,38] For a more comprehensive summary of the development and applications of the HABP assay, see de la Motte and Drazba.[35]

Although the HABP assay is used to visualize HA in different tissues, a rigorous optimization of fixation conditions across different tissue types is lacking. Such a study is critical because HA detection can vary with fixation conditions.[35,36,39] This fixative sensitivity is in part due to the unique properties of HA: unlike other glycosaminoglycans, HA is not typically covalently linked with any proteins integrated into the ECM and is thus more prone to wash out during fixation.[35] A review of the literature demonstrated that histochemical detection of HA has been performed in cells and tissues from several species, such as the mouse pancreas,[40] human skin,[39] human colon,[35] and mouse cumulus cells.[41] In these studies, five different fixatives were used, including Bouin's Solution, Carnoy's Solution, Ethanol-Formalin-Glacial Acetic Acid (EFG; 70%, 10%, 5% v/v, respectively), Histochoice, and 10% Neutral Buffered Formalin. Our study was designed to evaluate these commonly used fixatives and choose the one which allowed for the best matrix HA detection—both with regard to content and localization—via the HABP assay in parallel using histologic sections from three different tissues where HA is being actively investigated: ovary, kidney, and liver. We also included Modified Davidson's Solution given its wide use as a fixative in histological studies in tissues including the ovary, testes, and eye.[42,43] Therefore, the goal of this study was to identify the best fixative for HA detection (content and localization) in each organ from the 6 we chose based on previously published literature. A complete list of the fixatives used in this study, their compositions, species, and tissue type in which they were previously tested, and reference to previous work is found in Table 1.

Materials and Methods

Animals and Organ Harvest

Reproductively adult female CB6F1 mice (6–8 weeks old) were obtained from Envigo (Madison, WI). Our laboratories study female reproductive aging; thus, we exclusively use female mice. All mice were housed in a controlled barrier facility at Northwestern University's Center for Comparative Medicine on the Chicago Campus under constant temperature, humidity, and light (14 hr light/10 hr dark). Food and water were provided *ad libitum*. All animal experiments described here were approved by the Institutional Animal Care

Table 1. Fixatives Used in This Study and Their Composition.

Fixative Name	Fixative Components (%)	Species	Tissue Type	References
Bouin's Solution	Water (86.6%) Formaldehyde (9.2%) Acetic acid (4.9%) Methyl acohol (3.7%) Picric acid (0.6%)	Mouse	Cumulus cells in preovulatory follicles	Williams and Stanley[41]
Carnoy's Solution	Chloroform (43.2%) Ethyl alcohol (42.2%) Acetic acid (10.2%) Isopropyl alcohol (2.3%) Methyl alcohol (2.1%)	Mouse	Pancreas	Hull et al.[40]
Ethanol-Formalin-Glacial Acetic Acid	Ethyl alcohol (70%) Formalin (10% of 35% soln) Water (15%) Glacial acetic acid (5%)	Human	Skin from 35-year-old male	Lin et al.[39]
Histochoice[a]	Water (37.5–42.5%) Ethyl alcohol (25–50%) Isopropyl alcohol (2.5–10%) Glyoxal (<2.5%)	Mouse	Colon	de la Motte and Drazba[35] and Kessler et al.[44]
Modified Davidson's Solution	Water (42.2%) Formalin (37.5%) Ethyl alcohol (14%) Glacial acetic acid (6.3%)	Rat	Testes	Latendresse et al.[43]
10% Neutral Buffered Formalin	Water (94–95%) Formaldehyde (3.5–4%) Methyl alcohol (1.2%) Sodium phosphate dibasic (<1%)	Human	Skin from 35-year-old male	Lin et al.[39]

[a]Exact formulation is proprietary.

and Use Committee (Northwestern University) and were performed in accordance with National Institutes of Health Guidelines. Both ovaries (right and left), both kidneys (right and left), and the left lateral lobe of the liver were isolated from each animal. Ovaries were removed from the bursa and 3-mm-thick cross-sectional disks from the center of each kidney and liver were prepared. Organs were rinsed in phosphate buffered saline (PBS; Cat. #BP2944100, Fisher Scientific, Waltham, MA) and fixed as described below. To create an assay-positive control, mice were exposed to carbon tetrachloride, intraperitoneally. Carbon tetrachloride is a potent hepatotoxin which results in hepatocyte necrosis in the pericentral region of the liver and in which HA accumulates during liver regeneration; mice were euthanized 48 hr later.[37,45,46]

Tissue Fixation, Processing, Embedding, and Sectioning

Whole organs (ovaries) or pieces of each organ (kidney and liver) were pooled from individual mice to eliminate any potential animal-specific effects and randomly distributed across the six fixatives, with two to three organs per fixative. The fixatives were as follows: Bouin's Solution (Cat. #112032; Ricca Chemical Company, Arlington, TX), Carnoy's Solution (Cat. #R18510004C; Ricca Chemical Company), EFG, Histochoice (Cat. #H2904-1L; Sigma Aldrich, St. Louis, MO), 10% Neutral Buffered Formalin (Cat. #SF100-4; Fisher Scientific, Hampton, NH), and Modified Davidson's Solution (Cat. #64133-50; Electron Microscopy Sciences, Hatfield, PA) (Table 1). EFG was made immediately before tissue harvest with 70% 200-proof ethanol, 10% formalin solution (37% formaldehyde solution, Cat. #BP531-500; Fisher Scientific), 5% glacial acetic acid (Cat, #A38S-500; Fisher Scientific), and 15% MilliQ water (all v/v). Whole ovaries were fixed in a 1 mL volume, and liver slices and kidney disks (2 mm thick for both) in 4 and 7 mL volumes, respectively. Livers from carbon tetrachloride-exposed mice were cut as described above but only fixed in 10% Neutral Buffered Formalin. Once in the fixatives, samples were placed on a rocker at room temperature for 6 hr. Samples were then moved to 4C and gently rocked overnight. Following fixation, the tissues were rinsed in 70% ethanol three times and stored in 70% ethanol at 4C until processing

(24–48 hr later). Samples were then processed at the same time using an automated tissue processor (Leica Biosystems, Buffalo Grove, IL), which included dehydration, clearing, and infiltration of paraffin wax to preserve tissue structure per standard processing protocols. Samples were then all embedded into paraffin wax blocks using a Leica embedding station (Leica Biosystems). The paraffin-embedded tissue blocks were sectioned at the University of Kansas Medical Center Histology Core, and 5-μm-thick sections were mounted on slides for histological staining and analysis.

Hematoxylin and Eosin (H&E) Staining

To examine tissue architecture, ovary, kidney, and liver sections were stained with hematoxylin and eosin (H&E) using a Leica Autostainer (Leica Biosystems). All slides were stained using the same batch of reagents and at the same time. In brief, paraffin-embedded tissue sections were deparaffinized using xylene and rehydrated in a graded ethanol series (decreasing; 100%, 90%, 80%, ending in water). Slides were then stained with hematoxylin and rinsed before treating with a weakly alkaline solution (Bluing Reagent). Slides were rinsed, stained with eosin, and dehydrated following another series of ethanol baths (80%, 95%, and 100%). Finally, tissue was cleared with xylene and mounted with Cytoseal XYL (Cat. #831204; Fisher Scientific).

HABP Assay

Tissue sections were deparaffinized with two Citrisolv incubations (3 min each), then rehydrated in a graded alcohol series of 100%, 95%, and a second 95% incubation (for 2 min, 1 min, and 2 min, respectively). Slides were then washed in deionized water for 1 min followed by a 10-min wash on a rocker in 1X PBS. Endogenous avidin and biotin were blocked using the Avidin/Biotin Blocking Kit (Cat. #SP-2001; Vector Laboratories, Burlingame, CA). Avidin was applied first and allowed to incubate for 15 min in a humid chamber at room temperature. After avidin was decanted and slides were submerged in 1X PBS, biotin was applied for a 15-min incubation in a humid chamber at room temperature. Subsequently, sections were incubated with normal goat serum (Cat. #16-210-064; Fisher Scientific) for 20 min at room temperature in a humid chamber. Thereafter, negative control sections were incubated for 1 hr at 37C with 1 mg/mL hyaluronidase (Cat. #H3884-100MG; Sigma-Aldrich, St. Louis, MO) in normal saline, which was used as a specificity control for HA signal. Hyaluronidase is the enzyme that digests HA, so this treatment should abrogate fluorescent signal in the tissue. Experimental samples and positive control sections were incubated in saline alone at 37C for 1 hr. After washing in PBS, biotinylated-HABP (Cat. #38599; Calbiochem, San Diego, CA) diluted in normal goat serum was applied to all sections (experimental samples as well as positive and negative controls) for a 1-hour incubation, at room temperature. Using a separate set of all slides for all three organs, we repeated the HABP assay using *Streptomyces hyaluronlyticus* hyaluronidase (Millipore Sigma, catalog # 389561-100U). Sections were incubated with 50 U/mL *Streptomyces* hyaluronidase in a 20 mM sodium acetate, 75 mM sodium chloride buffer, pH 6.0 for 24 hr at 37C; serial sections were incubated with the buffer alone for the same duration and at the same temperature. Slides were then washed with 1X PBS. The signal was amplified first by incubating the slides in Vectastain Elite ABC reagent for 30 min (Cat. #PK-6101; Vector Laboratories) and then by tyramide signal amplification by incubating with TSA reagent at 1:400 dilution using the TSA Plus Fluorescein System for 5 min (Cat. #NEL741001KT; Perkin Elmer, Waltham, MA); both incubations took place in a humidity chamber and at room temperature. A third complete set of slides was treated the same as the bovine testicular hyaluronidase-treated slides, only no HABP was applied to the sections. This control was included to rule out fixative-specific autofluorescence. Samples were mounted in Vectashield HardSet Antifade Mounting Medium with DAPI (4′,6-diamidino-2-phenylindole; Cat. #H-1500; Vector Laboratories) to stain cell nuclei. All histological organ sections were processed in parallel so that all conditions for a specific organ could be directly compared. The HABP assay was performed on two biological replicates from each fixative and an assay positive control (liver from carbon tetrachloride-exposed mice) was used with each HABP assay.

Imaging

H&E stained slides were imaged using brightfield microscopy. Histological sections of the ovary were scanned with a 20X objective using a EVOS FL Auto Imaging System (Thermo Fisher, Waltham, MA). Light settings were kept consistent throughout scanning. Secondary follicles in H&E stained slides were imaged using a 40X objective. Epifluorescence imaging of HABP-stained ovary sections was also performed using an EVOS FL Auto Imaging system equipped with the following LED light cubes: Green fluorescent protein (GFP) (Ex 470/22 nm; Em 510/42 nm)

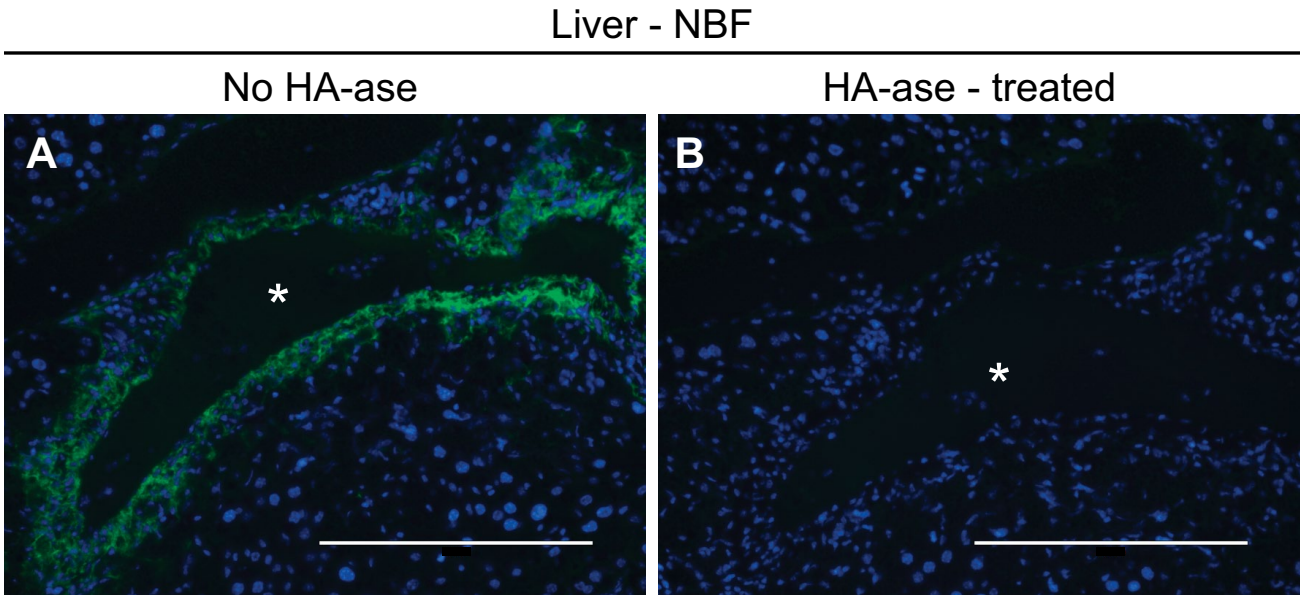

Figure 1. Hepatotoxin-induced hepatic hyaluronan production produces a robust positive control for the HABP assay. Carbon tetrachloride was injected into C57BL/6 mice and livers were collected 48 hr later and fixed using neutral buffered formalin (NBF). (A) The HABP assay revealed robust hyaluronan accumulation in the injured regions around hepatic central veins (asterisk) during the repair phase after carbon tetrachloride exposure. (B) Bovine testicular hyaluronidase treatment of serial sections prevented detection of hyaluronan. Scale bars are 200 μm. Abbreviation: HABP, Hyaluronan binding proteins.

and DAPI (Ex 357/44 nm; Em 447/60 nm). For liver and kidney sections, HA-specific (GFP) and DAPI fluorescence were captured using an Olympus BX51 microscope, Olympus BH2RFLT3 burner, Olympus DP71 camera, and DP Controller software (Olympus, Waltham, MA) using 4X, 10X, and 20X objectives. The imaging settings were determined based on the most intense HA signal for each tissue among the 6 different fixatives on each objective (EFG and Carnoy's Solution in the ovary and EFG in the liver and kidney). These settings were kept consistent for the same tissue type across all experimental conditions including the controls (hyaluronidase-treated tissue). DAPI settings were adjusted to visualize nuclei. Optimal fixation conditions for the ovary, kidney, and liver were determined by examining relative HABP staining intensity and localization across all fixative conditions for each organ. Analyses were confirmed by board certified pathologists for the kidney and liver.

Results

Generation of a Robust HABP Assay Positive Control

Identifying good positive controls for histochemical analyses is critical for accurate interpretation of staining results, including for the HABP assay. In separate studies, we discovered that HA accumulates in the injured pericentral regions of mouse liver 48 hr after carbon tetrachloride exposure in mice[37] (Fig. 1A). Specificity of our HABP protocol was confirmed as no HA signal was detected in bovine testicular hyaluronidase-treated serial sections (Fig. 1B). Therefore, we chose this tissue as our assay positive control. Serial sections from this same block were used as positive controls for HABP staining of the ovary, kidney, and (uninjured) liver as described below.

EFG and Carnoy's Solution Fixation Are Optimal for Detection of Ovarian HA

We first used H&E staining to evaluate and compare the preservation of ovarian architecture across fixation conditions (Figs. 2 and 3). H&E staining is one of the principal staining methods used to evaluate tissue architecture, whereby hematoxylin stains nucleic acids (i.e., cell nuclei) deep blue and eosin stains cytoplasmic proteins pink.[47] As evident in whole ovary sections, key ovarian structures and morphology were well-preserved with each fixative (Fig. 2). The follicle is the functional unit of the ovary consisting of an oocyte surrounded by its companion granulosa cells. Follicles at various stages of development were clearly visible within the ovarian stroma in each ovarian section (Fig.

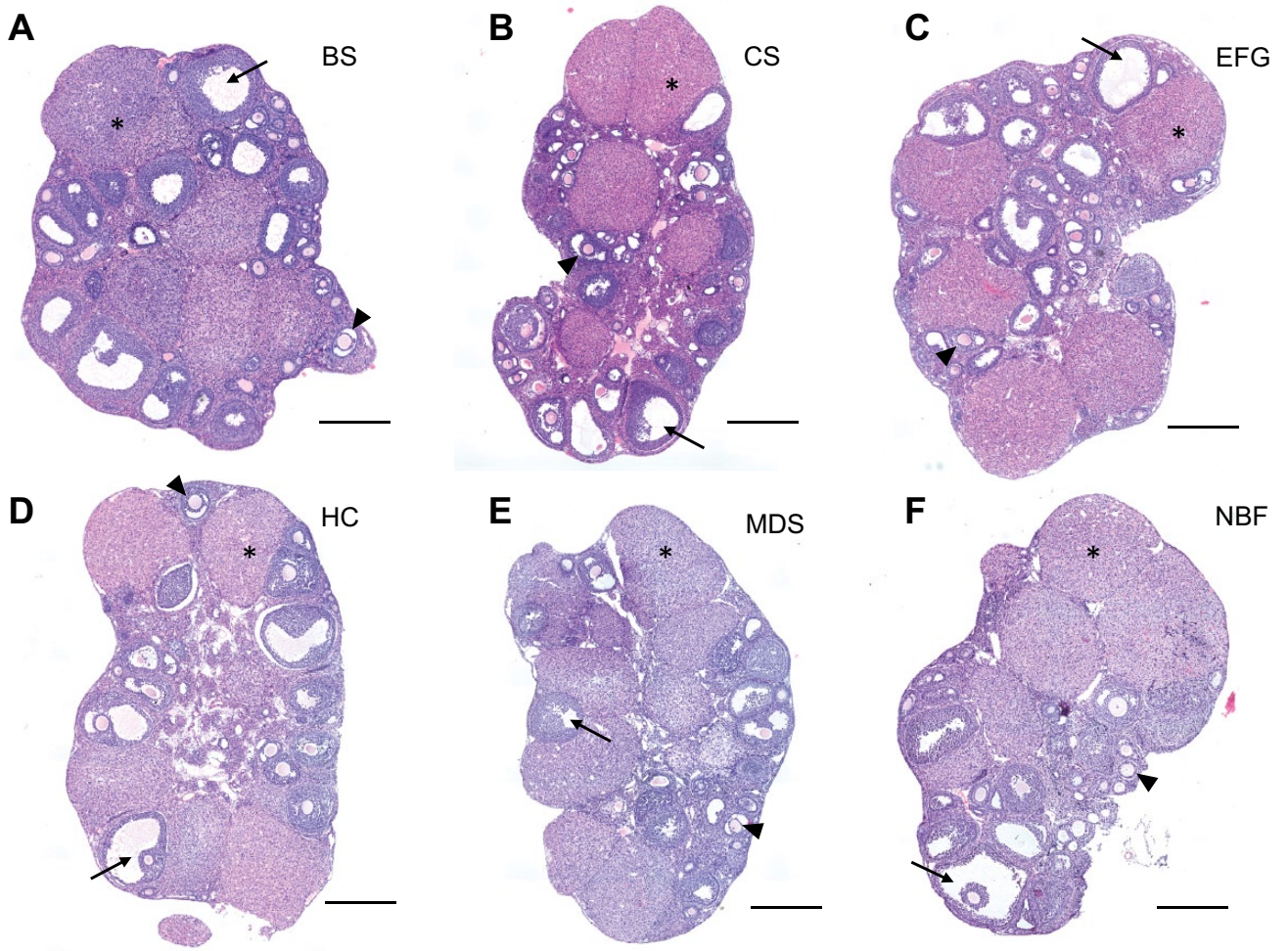

Figure 2. Hematoxylin and eosin–stained whole ovary tissue sections reveal adequate tissue architecture preservation across fixatives. Representative H&E-stained images of whole ovary tissue sections fixed in (A) Bouin's Solution (BS), (B) Carnoy's Solution (CS), (C) Ethanol-Formalin-Glacial Acetic Acid (EFG), (D) Histochoice (HC), (E), Modified Davidson's Solution (MDS), and (F) 10% Neutral Buffered Formalin (NBF). H&E staining was performed at the same time for all fixatives. Ovarian sub-structures such as early developing follicles (arrowhead), antral cavities of mature follicles (arrow), and corpora lutea (asterisk [*]) are indicated in each section. EFG and Carnoy's Solution fixation resulted in more prominent eosinophilic staining as compared to other fixative conditions, as shown by pink staining. Scale bars are 400 μm.

2). Compared to the other fixatives tested, EFG and Carnoy's Solution fixations resulted in more prominent eosinophilic staining, which provides optimal contrast between different cell types in the ovary (Fig. 2B and C). This is particularly evident in the corpora lutea, which are the endocrine-producing structures formed from follicles following ovulation (Fig. 2B and C). The corpora lutea are composed of hypertrophied luteinized granulosa cells, which contain a larger cytoplasmic-to-nuclear ratio. As a result, the corpora lutea are typically more eosinophilic, and this is best preserved with EFG and Carnoy's Solution compared to Bouin's Solution, Histochoice, Modified Davidson's Solution and 10% Neutral Buffered Formalin (Fig. 2B, C vs. A, D, E, F). Eosinophilic staining was also more pronounced in the higher magnification images of early stage follicles referred to as secondary follicles in EFG and Carnoy's Solution-fixed ovaries when compared to the other fixatives (Fig. 3B and C). With these fixatives, vital follicle structures including the theca cell layer are more easily discernible from the surrounding ovarian stroma (Fig. 3B and C insets). Theca cells, identifiable by their long spindle shape, surround growing follicles and are essential for sex steroid hormone production.[48]

We then investigated HA distribution in ovarian tissue sections from the same experimental samples using the HABP assay.[37] In ovarian sections, the HABP signal was consistently most intense in Bouin's Solution, Carnoy's Solution, and EFG fixation

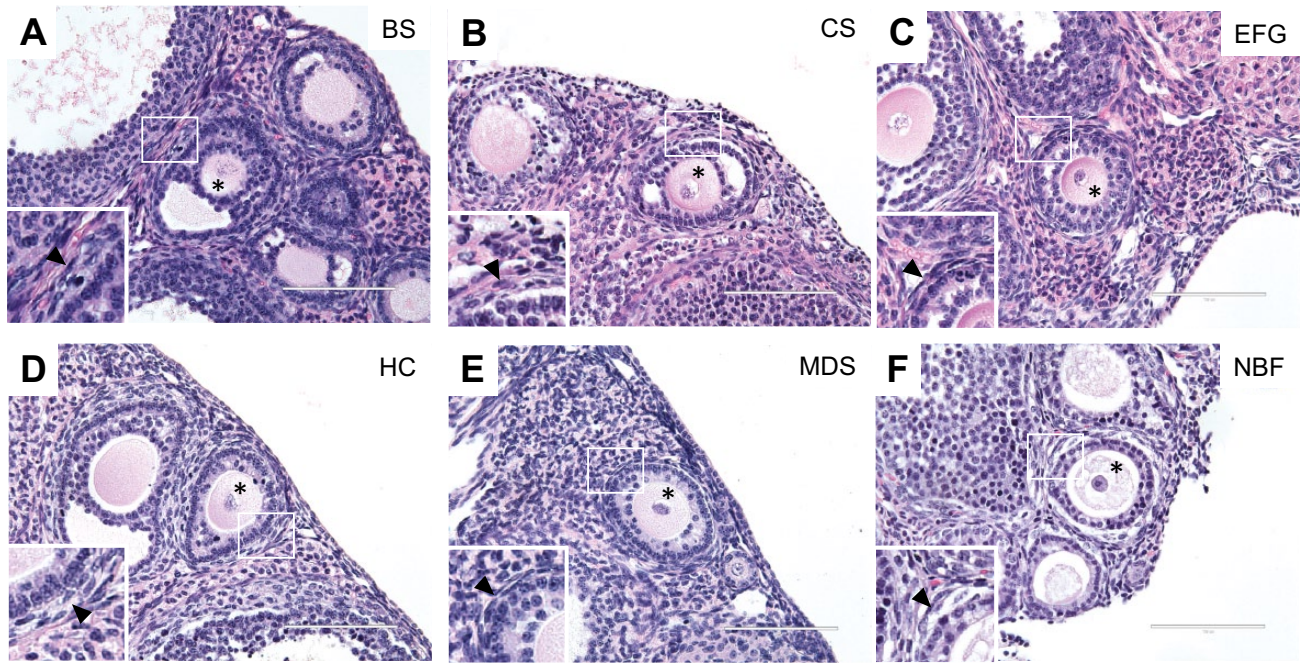

Figure 3. Hematoxylin and eosin staining of ovarian tissue sections containing secondary follicles highlight differences in eosinophilic staining between fixatives. Representative H&E images of secondary follicles in ovarian tissue fixed in (A) Bouin's Solution (BS), (B) Carnoy's Solution (CS), (C) Ethanol-Formalin-Glacial Acetic Acid (EFG), (D) Histochoice (HC), (E) Modified Davidson's Solution (MDS), and (F) 10% Neutral Buffered Formalin (NBF) reveal increased contrast due to greater eosinophilic staining in EFG and Carnoy's Solution-fixed ovarian sections, as shown by pink staining (note that H&E staining occurred concurrently ovary sections from all fixatives). Further, sub-follicular structures such as the oocyte (asterisk [*]) and theca cells (insets, arrowhead), which surround growing follicles and produce steroid hormones, are preserved across all fixation conditions. Scale bars are 100 μm.

conditions compared to Histochoice, Modified Davidson's Solution and 10% Neutral Buffered Formalin (Fig. 4A to C vs. D to F). All of the observed signals in ovarian tissue were specific to HA, as signal was abrogated following incubation with bovine testicular hyaluronidase (Fig. 4, insets), or Streptomyces hyaluronidase (Supplemental Fig. 3A, inset). In all fixative conditions, the HA signal was visible in the follicular fluid of antral follicles. Antral follicles, which are the most mature follicle stage, possess a cavity filled with follicular fluid (visible as white spaces in the histological sections), and this fluid contains high HA concentrations (Figs. 2, 4 and 5).[49] Thus, these findings validate the HABP assay for ovarian HA detection. Interestingly, however, only fixation with Bouin's Solution, Carnoy's Solution, and EFG revealed prominent HA localization in the theca layer surrounding growing follicles (Fig. 4A to C). At a higher magnification, the localization of HA at the theca layer was clearly visible around early antral follicles in EFG and Carnoy's Solution-fixed ovarian sections (Fig. 5B and C). This signal was less intense in the Bouin's Solution-fixed tissue, and the DAPI signal was also more diffuse with this fixative, making finer tissue structures less visible (Fig. 5A). Thus, based on these overall findings, of the fixatives chosen for this analysis, EFG and Carnoy's Solution are optimal fixatives for visualization of HA in the murine ovary (Table 2).

Fixation Did Not Appreciably Alter Kidney HABP Detection

The kidney is a highly complex organ with several anatomically and functionally distinct segments (Supplemental Fig. 1). H&E staining is commonly used for morphological analysis of kidney tissue. Under ideal staining conditions, different regions of the kidney (cortex, outer stripe of the outer medulla, inner stripe of the outer medulla and inner medulla) can be readily observed. Therefore, we examined how different fixatives affected both preservation of the distinct regions of the kidney as well as H&E staining intensity (as in the ovarian H&E studies described above). Among the different fixatives tested, EFG provided the best staining contrast, allowing for recognition of all major kidney regions (Fig. 6C, Supplemental Fig. 1). While the cortex could

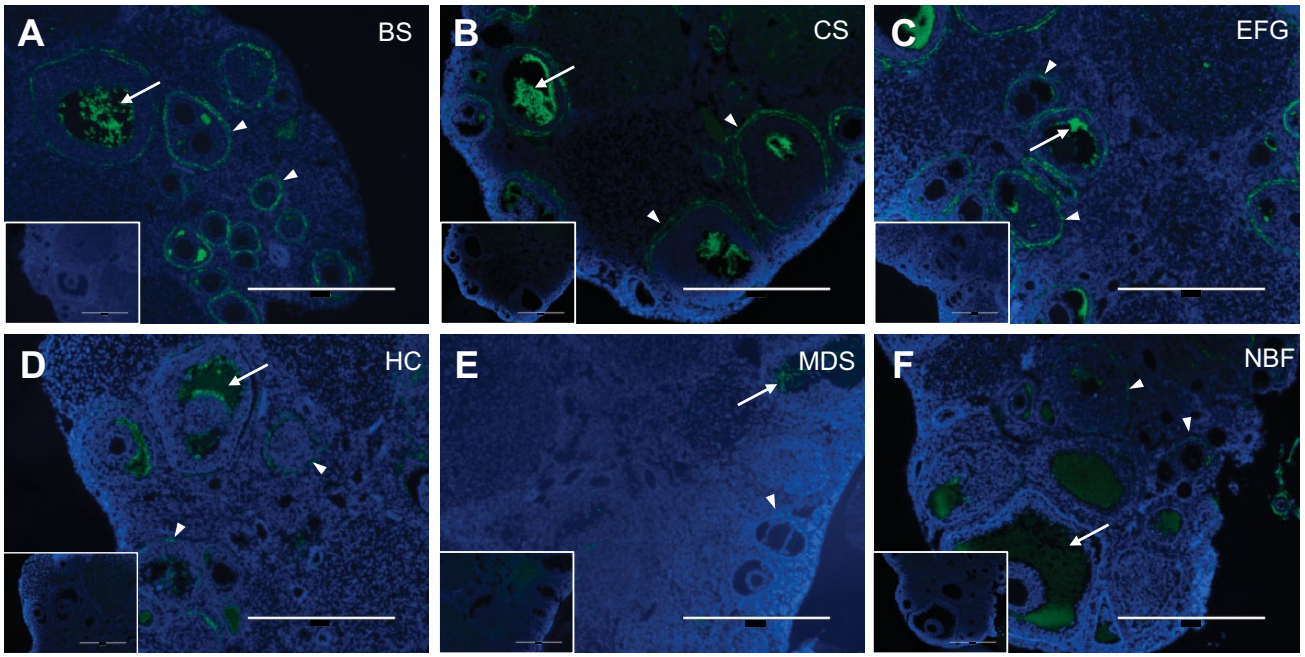

Figure 4. Ethanol-Formalin-Glacial Acetic Acid, Carnoy's Solution, and Bouin's Solution produce optimal HABP signal at low magnification in the ovary. Representative images of HABP-stained ovarian tissue fixed in (A) Bouin's Solution (BS), (B) Carnoy's Solution (CS), (C) Ethanol-Formalin-Glacial Acetic Acid (EFG), (D) Histochoice (HC), (E) Modified Davidson's Solution (MDS), and (F) 10% Neutral Buffered Formalin (NBF). For all images, DNA is shown in blue and HA is shown in green. HA shows greatest localization in the follicular fluid of antral follicles (arrow) as well as in the layer of theca cells immediately surrounding growing follicles (arrowhead). Fixation with EFG, Carnoy's Solution, and Bouin's Solution produced greater HA signal brightness. Negative controls showing sections treated with bovine testicular hyaluronidase, which degrades HA and abrogates HABP signal, are shown in the insets. Scale bars are 400 μm.

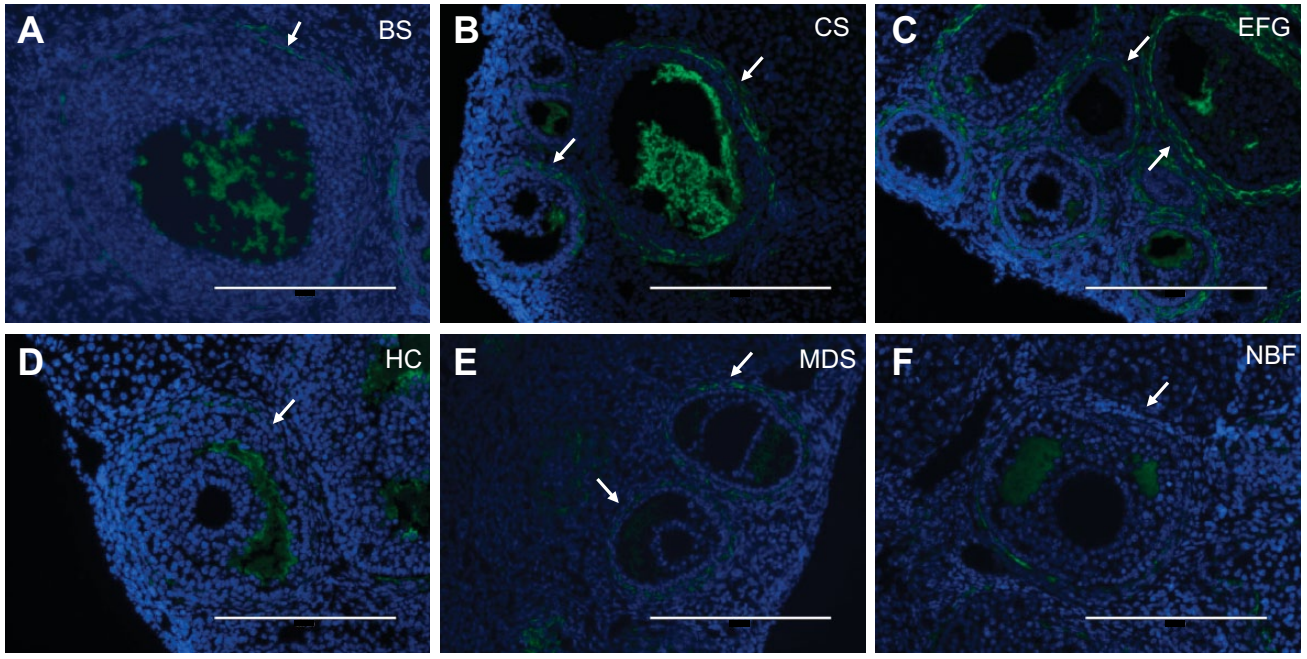

Figure 5. Ethanol-Formalin-Glacial Acetic Acid and Carnoy's Solution produce superior HA localization preservation in the theca cell layer surrounding ovarian follicles. Representative images of HABP-stained ovarian tissue fixed in (A) Bouin's Solution (BS), (B) Carnoy's Solution (CS), (C) Ethanol-Formalin-Glacial Acetic Acid (EFG), (D) Histochoice (HC), (E) Modified Davidson's Solution (MDS), and (F) 10% Neutral Buffered Formalin (NBF). For all images, DNA is shown in blue and HA is shown in green. Both EFG and Carnoy's Solution fixation best preserve and detect HA localization to the theca layer of cells surrounding growing follicles (arrows). Scale bars are 200 μm.

Table 2. Summary of Relative Effectiveness of Fixation Conditions for the HABP Assay in Ovary, Kidney, and Liver Tissue.

Fixative	Ovary	Kidney	Liver
Bouin's Solution	++	+++	+
Carnoy's Solution	+++	+++	+++
Ethanol-Formalin-Glacial Acetic Acid	+++	+++	+++
Histochoice	+	+++	+
Modified Davidson's Solution	+	++	++
10% Neutral Buffered Formalin	+	+++	++

+++Optimal. ++ Acceptable. + Poor.

be easily distinguished from the medulla in H&E stained sections from kidneys fixed with Bouin's Solution, Carnoy's Solution, or Histochoice (Fig. 6A, B and D), individual sub-regions of the kidney (outer stripe of the outer medulla, inner stripe of the outer medulla and inner medulla) could not be as easily identified. All other fixatives interfered with the identification of these regions (Fig. 6E and F). With regard to staining intensity, fixation with Bouin's Solution, Carnoy's Solution, and EFG intensified eosinophilic staining (Fig. 6A to C), but all tested fixatives sufficiently preserved kidney tissue integrity, allowing for identification of different structures (i.e., glomeruli and tubules) through histological analysis (Fig. 7). As an example, glomeruli and proximal or distal convoluted tubules are annotated in Figure 7A. Taken together, and within the experimental conditions of this study, EFG-fixed kidney tissue produces optimal H&E staining contrast and intensity, allowing for

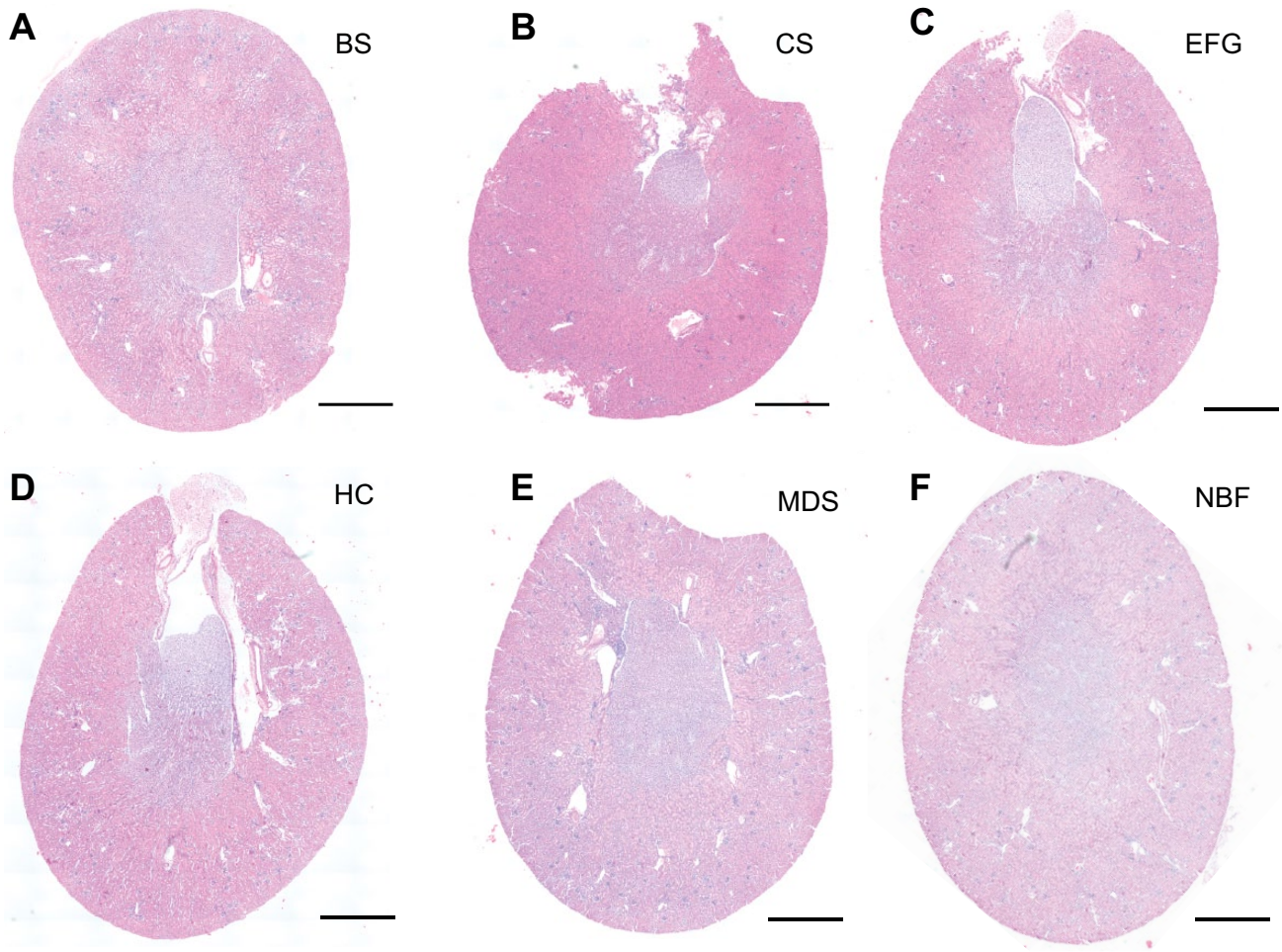

Figure 6. Fixation with Bouin's Solution, Carnoy's Solution, and Ethanol-Formalin-Glacial Acetic Acid produce eosinophilic staining in whole kidney sections. Low power representative images from cross-sectioned kidneys stained with H&E, at the same time, following fixation in (A) Bouin's Solution (BS), (B) Carnoy's Solution (CS), (C) Ethanol-Formalin-Glacial Acetic Acid (EFG), (D) Histochoice (HC), (E) Modified Davidson's Solution (MDS), and (F) 10% Neutral Buffered Formalin (NBF). Kidney regions such as cortex, outer stripe of the outer medulla, inner stripe of the outer medulla, and inner medulla are best seen with EFG fixation. However, the cortex and the medulla can be distinguished from one another in sections fixed with Bouin's Solution, Carnoy's Solution, or Histochoice. Among different fixatives, Bouin's Solution, Carnoy's Solution, and EFG produced more intense eosinophilic staining. Scale bars are 400 μm.

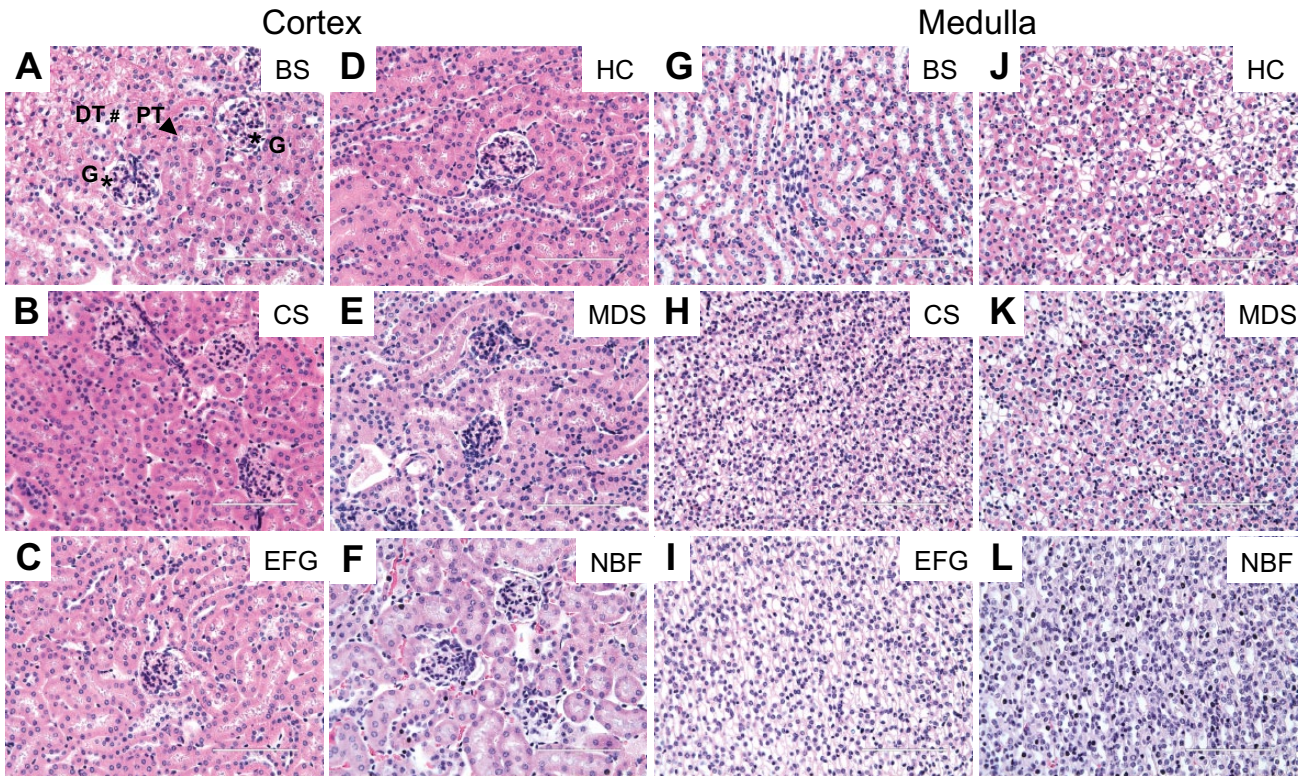

Figure 7. Acceptable quality of hematoxylin and eosin staining in kidney tissue across fixative conditions despite variations in eosinophilic staining. Shown are representative H&E images of kidney cortex and medulla tissue fixed in (A, G) Bouin's Solution (BS), (B, H) Carnoy's Solution (CS), (C, I) Ethanol-Formalin-Glacial Acetic Acid (EFG), (D, J) Histochoice (HC), (E, K) Modified Davidson's Solution (MDS), and (F, L) 10% Neutral Buffered Formalin (NBF). All staining was performed at the same time. While fixation with Bouin's Solution, Carnoy's Solution, and EFG intensified eosinophilic staining, the quality of H&E staining was overall acceptable across different fixatives allowing preservation of different structures in the kidney. For example, glomeruli (G, asterisk [*]), proximal convoluted tubules (PT, arrowhead), and distal convoluted tubules (DT, hash sign [#]) are indicated. Scale bars are 100 μm.

visualization of all major regions of the kidney as well as of micro-structures such as glomeruli and tubules.

Similar to the ovarian studies described above, we next determined how different fixatives affected detection of HA in kidney tissue using the HABP assay. In the healthy kidney, HA is found at relatively low levels in the cortex.[50] Indeed, HA localization in the kidney cortex was limited to the periarteriolar space in all fixative conditions (Fig. 8). Furthermore, as has been previously reported, HA was abundantly found in the interstitium of the medulla, with diffuse interstitial HA signal in the outer stripe of the outer medulla and inner medulla (Fig. 8, Supplemental Fig. 2).[50] Pre-treatment of serial sections with bovine testicular hyaluronidase (Fig. 8, Supplemental Fig. 2, insets) or with Streptomyces hyaluronidase (Supplemental Fig. 3C, inset) abrogated the HA signal. Thus, all fixatives tested consistently preserved HA distribution in kidney tissue, although the HA signal was weakest with Modified Davidson's Solution fixation (Fig. 8K) (Table 2).

EFG and Carnoy's Solution Fixation Are Optimal for Detection of Hepatic HA

To evaluate the effectiveness of each fixative in liver, we performed H&E staining on sections as done for the ovary and kidney. Bouin's Solution, Carnoy's Solution, and EFG preserved liver architecture and limited histological artifacts (e.g., cracking and tearing) (Figs. 9A to C and 10A to C), whereas Histochoice and Modified Davidson's Solution compromised the tissue integrity throughout the section (Figs. 9D and E and 10D and E); tissue cracking was less pronounced in liver sections fixed in 10% Neutral Buffered Formalin (Figs. 9F and 10F). Interestingly, only Neutral Buffered Formalin preserved eosinophilic staining of red blood cells (Fig. 10F). Of the fixatives tested, Carnoy's Solution produced the most saturated staining with H&E, preserving the eosinophilic nature of the mitochondria-rich hepatocyte cytoplasm and glycogen, and was deemed the best fixative for histological analysis in our study (Figs. 9B and 10B).[51,52]

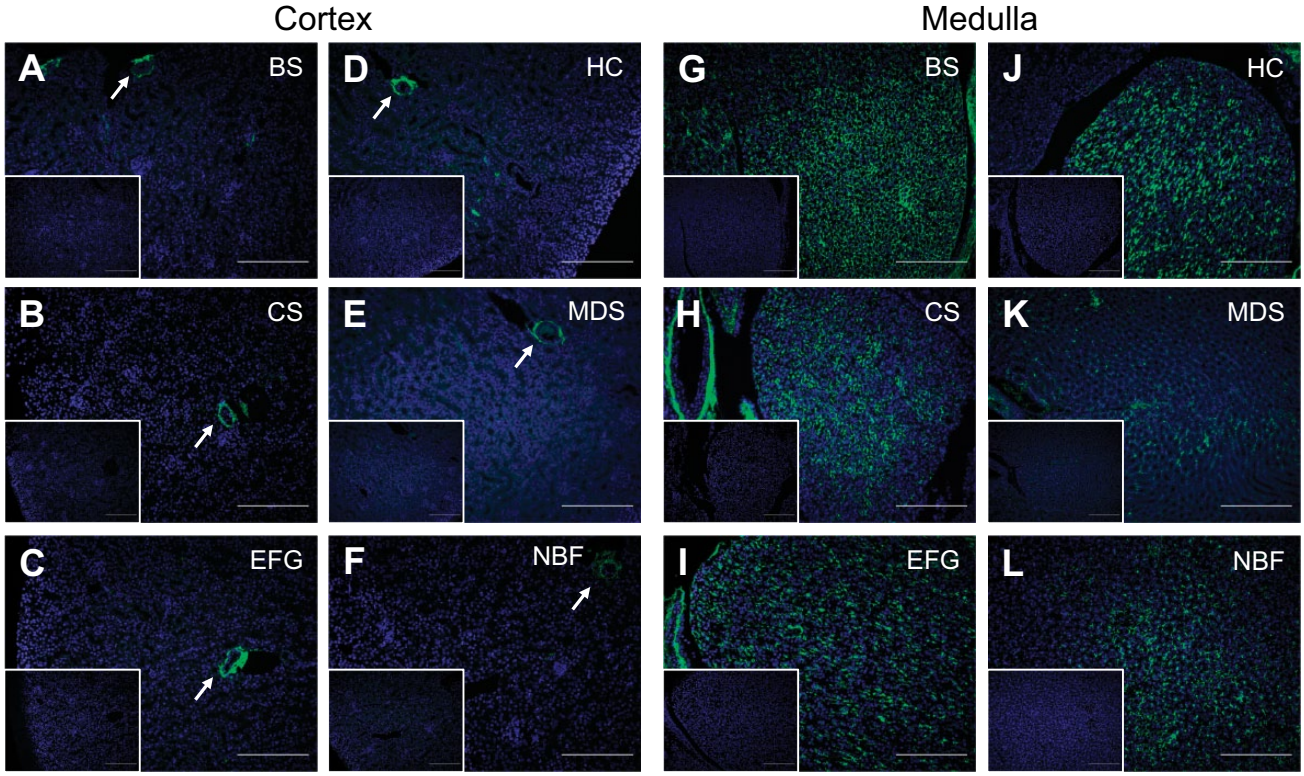

Figure 8. Kidney hyaluronan localization is least sensitive to fixative choice. Representative images of HABP-stained kidney tissue following fixation in (A, G) Bouin's Solution (BS), (B, H) Carnoy's Solution (CS), (C, I) Ethanol-Formalin-Glacial Acetic Acid (EFG), (D, J) Histochoice (HC), (E, K) Modified Davidson's Solution (MDS), and (F, L) 10% Neutral Buffered Formalin (NBF). For all images, DNA is shown in blue and HA is shown in green. All fixatives consistently preserved and allowed for HA detection in kidney tissue, although HA signal was weakest with Modified Davidson's Solution fixation. Specifically, kidney cortex showed HA localization limited to the periarteriolar space while there was diffuse interstitial HA signal in the medullary region. Arrows indicate cortical HA-positive periarteriolar regions. Negative controls showing sections treated with bovine testicular hyaluronidase are shown in insets. Scale bars are 20 μm. Abbreviations: HABP, Hyaluronan binding proteins; HA, hyaluronan.

We next evaluated our ability to detect HA in the liver using the HABP assay. The uninjured liver is an HA-poor organ when compared to other organs.[30] The only positive HA staining routinely found in healthy mouse liver is associated with the peribiliary region (i.e., the region immediately surrounding branches of the biliary tree/bile ducts), but this observation was fixative-specific (Fig. 10G to L). We found greatest peribiliary HA recovery when livers were fixed in Carnoy's Solution or EFG (Fig. 10H and I) and limited recovery when livers were fixed in Modified Davidson's Solution or 10% Neutral Buffered Formalin (Fig. 10K and L); in our hands, no HA was found in livers fixed in Bouin's Solution or Histochoice (Fig. 10G and J). To confirm specificity of the HABP assay, serial sections were pretreated with bovine testicular hyaluronidase (Fig. 10, insets, and Fig. 1) or Streptomyces hyaluronidase (Supplemental Fig. 3E, inset) prior to incubating with biotinylated HABP. Taken together, these data suggest that, when evaluating the fixatives used in this study, EFG and Carnoy's Solution are the optimal fixatives for preserving HA in healthy liver tissue (Table 2).

Discussion

Our study is unique as it is the first to demonstrate tissue-specific outcomes for the HABP assay across 6 defined fixatives and fixation conditions and between 3 organs all performed using the same, healthy mice, and at the same time. It is important to note that we do not claim that our findings will apply to other organs tested with the same fixatives. However, given the previously published literature demonstrating a unique ability of alcohol-based fixatives to allow for greater HA detection in the HABP assay, it is not unreasonable to predict this would be the case, but should not be assumed. Importantly, and because tissues tend to differ with respect to the relative concentration of different macromolecules they contain, it is imperative that each laboratory performs a rigorous test of fixatives (and

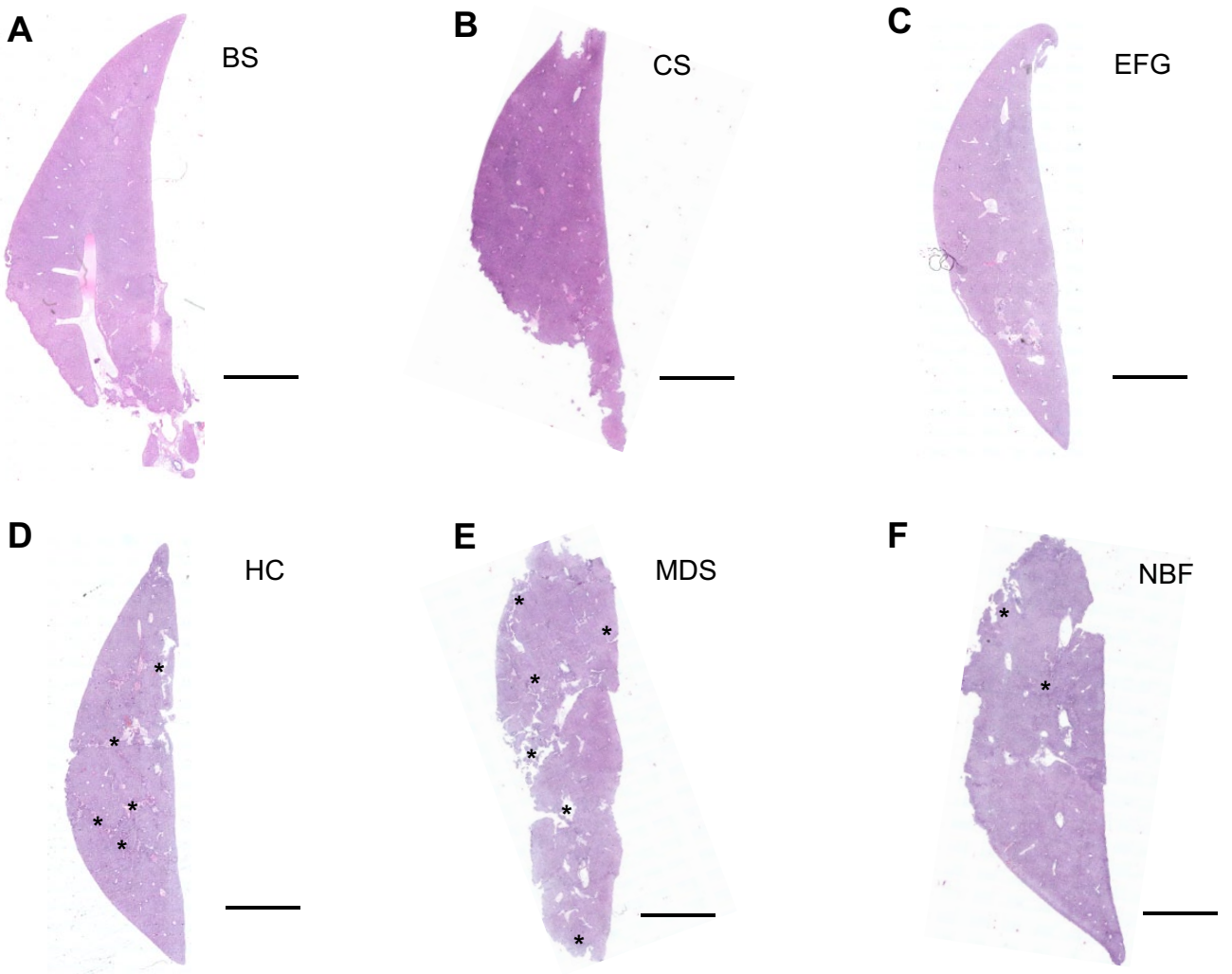

Figure 9. Hematoxylin and eosin-stained whole liver tissue sections reveal optimal tissue architecture preservation after fixation in Bouin's Solution, Carnoy's Solution, and Ethanol-Formalin-Glacial Acetic Acid. H&E staining (performed at the same time for all fixatives) was used to evaluate healthy liver tissue architecture after fixing in (A) Bouin's Solution (BS), (B) Carnoy's Solution (CS), (C) Ethanol-Formalin-Glacial Acetic Acid (EFG), (D) Histochoice (HC), (E) Modified Davidson's Solution (MDS), and (F) 10% Neutral Buffered Formalin (NBF). Carnoy's Solution best preserved liver tissue architecture, while Bouin's Solution and EFG also sufficiently preserved liver tissue. Asterisks (*) indicate fixation/processing artifacts (D, E). Scale bars are 400 μm.

other variables) prior to initiating an analysis of HA content in various tissues.

Of note, choice of the best HA fixatives in ovary, kidney, and liver did not change with use of a second, more specific hyaluronidase derived from *Streptomyces hyaluronlyticus*, and omission of HABP did not reveal fixative-specific autofluorescence in any of the tissues (Supplemental Fig. 3), improving the rigor and reproducibility of our study. Neither of these control assays changed the results of our study. However, at the concentrations we used in this study, bovine testicular hyaluronidase can also degrade chondroitin sulfate, and those who wish to evaluate this proteoglycan in the same sections should consider *Streptomyces* hyaluronidase instead.

Our findings demonstrate that fixation can alter the ability to detect tissue-specific HA content, macro- and microstructure, as well as localization in tissues in situ, which is consistent with other studies.[35,36,39] EFG and Carnoy's Solution produced the most robust HABP assay signal of all fixations examined in the ovary and liver. However, in the kidney, while EFG and Carnoy's Solution produced excellent HA signal brightness and localization, only Modified Davidson's Solution provided less than optimal HA staining when compared to the other fixatives. Bouin's Solution, Histochoice, and 10% Neutral Buffered Formalin fixation rendered the HABP assay less sensitive to HA in the ovary and liver, as HA signal was produced in sub-organ structures with high

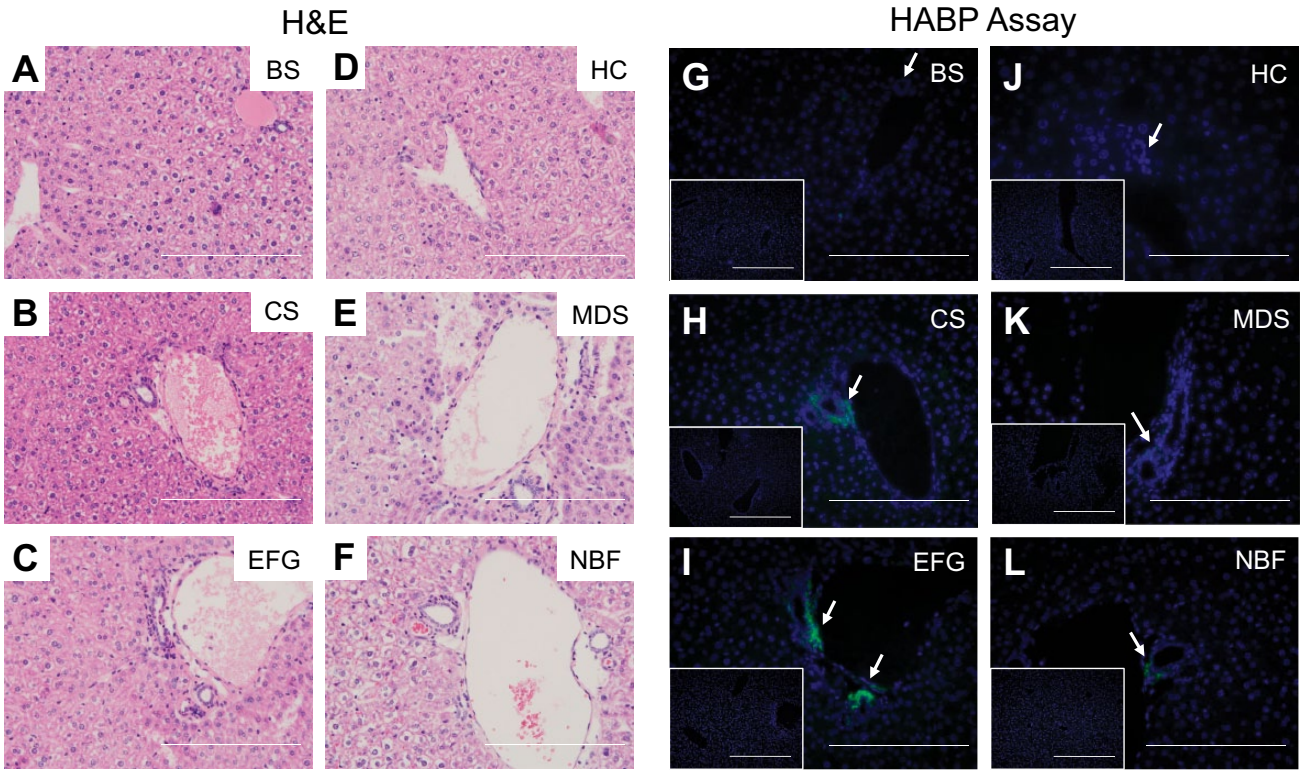

Figure 10. Ethanol-Formalin-Glacial Acetic Acid and Carnoy's Solution fixation produce superior HA preservation in the peribiliary regions of liver tissue. H&E staining (left) and the HABP assay (right) were used to compare the microanatomical architecture of the hepatic portal triad with HA localization and intensity in normal mouse livers fixed with (A, G) Bouin's Solution (BS), (B, H) Carnoy's Solution (CS), (C, I) Ethanol-Formalin-Glacial Acetic Acid (EFG), (D, J) Histochoice (HC), (E, K) Modified Davidson's Solution (MDS), and (F, L) 10% Neutral Buffered Formalin (NBF). DNA is shown in blue and HA is shown in green, and areas showing brightest HA signal are indicated with arrows. Negative controls showing sections treated with bovine testicular hyaluronidase are found as insets. Scale bars are 20 µm.

levels of HA (e.g., follicular fluid in antral follicles), but not in structures with lower levels of HA (e.g. theca layer surrounding developing follicles). Moreover, EFG and Carnoy's Solution both resulted in high-quality H&E staining in the ovary, kidney, and liver which allows for morphological assessment of tissue in parallel with the HABP assay. Furthermore, Bouin's Solution fixation also produced high quality H&E staining in the liver and kidney. However, given that different fixatives have different windows of optimal fixation and that these windows depend on the bioanalyte being investigated (protein, RNA, DNA, etc.), further fixation optimization could be performed to improve preservation of cell morphology, structure, and staining contrast and intensity for Bouin's solution, Modified Davidson's solution, and Neutral Buffered Formalin in ovary, kidney, and liver.[53]

Several authors have reported that alcohol-based fixatives, such as EFG and Carnoy's Solution, preserve HA far better than aldehyde-based fixatives such as 10% Neutral Buffered Formalin, though it is not fully understood why this is the case.[36,39] Among all glycosaminoglycans, HA is particularly prone to wash out during fixation, as it is typically not linked to any protein that can anchor it into the extracellular matrix.[35] Whereas HA probably leaches out during fixation, it likely continues to be lost during the dehydration and rehydration steps that tissues undergo during tissue processing onto glass slides in preparation for affinity-histochemistry, without these covalently linked proteins. This phenomenon appears to be diminished in alcohol-based fixatives. Taken together, our results demonstrate a conserved benefit of alcohol-based fixatives in HA detection using the HABP assay in three different organs.[35]

There are some limitations to this study. For example, we did not fix all possible organs in the chosen fixatives, so our data may not inform researchers which fixatives to consider in tissues outside of ovary, kidney, and liver. Also, the quality of one fixative may differ based on the reagent grade chosen. For example, it came to our attention after this study was complete that the Histochoice we chose in this study was less optimal

then the molecular biology grade of the same fixative (H2409 vs H120, the latter of which is the better of the two). In addition, many parameters could be further tested such as expanding the number of fixatives tested, and fixation times, or changing the HABP incubation durations to reveal staining not detected using the 1 hr incubation time used in this study. Furthermore, given that many researchers will perform staining procedures to localize HA in parallel with other molecules in the same tissue section, it would be imperative to re-optimize fixation, and other aspects of the staining procedure, to ensure that the fixatives which work best for HA localization do not negatively influence antibody binding. For example, others have reported on the effects of fixation on the immunoreactivity of key HABPs such as versican, tumor necrosis factor-stimulated genes 6 (TSG6) and IαI.[40] Furthermore, the appearance of co-localization of binding proteins such as versican with HA using immunofluorescence can be impacted by fixation condition.[36] Finally, although we employed two different hyaluronidases, a "no HABP" control, and a strong positive control, additional controls can be considered. One example of an additional negative control would be use of HABP after its overnight preincubation with HA.[39] Therefore, and based on the findings of our study, we would recommend that each laboratory perform their own rigorous assessment of fixation and staining techniques, including the careful consideration of negative and positive controls, and include an alcohol-based fixative when choosing the procedure best suited for their specific research needs.

Across all three tissues of interest, HA localization plays important roles in tissues under physiologic conditions. In the ovary, prominent HA signal was observed in the follicular fluid of antral follicles, as the somatic cells (called cumulus cells) surrounding the oocyte in antral follicles synthesize large quantities of HA.[49] This HA is then released into the extracellular matrix of the cumulus-oocyte-complex and the surrounding follicular fluid prior to ovulation.[54] Furthermore, EFG, Carnoy's Solution and Bouin's Solution fixation conditions revealed a previously unrecognized localization of HA to the theca layer of growing follicles. The role of HA in theca cell recruitment to growing follicles warrants additional investigation. In healthy kidney, EFG fixation demonstrated that HA is primarily found in the interstitium of the inner medulla and in smaller amounts in the outer medulla, while the cortex contains negligible amounts of HA except for around renal arterioles. This spatial distribution fits with the role of HA in regulation of fluid homeostasis.[50] During kidney development, HA acts as a driver of morphogenic branching and differentiation.[55] Specifically, high levels of HA accumulate in the ECM surrounding migrating and proliferating cells in the immature metanephros and decrease following differentiation and branching.[56] In the post-ischemic kidney, HA accumulates in the renal cortex and associates with interstitial edema,[57] while alterations in HA are noted in other kidney diseases, including diabetic nephropathy, kidney stones and graft rejection.[58] In the absence of injury or disease, we observe that liver HA is very low and localized to the peribiliary region following fixation with EFG or Carnoy's Solution.[30,59] While used as a biomarker for liver disease severity, few studies have examined hepatic HA localization.[60–64] However, those previous studies indicate that hepatic HA is superimposed on fibrotic/cirrhotic regions.[65] Interestingly, hepatic HA accumulation is a feature common to many liver diseases, although HA amount differs based on disease etiology. For example, alcohol-associated and non-alcohol-associated liver disease both exhibit robust HA accumulation, although the former is associated with greater HA and more progressive disease.[65]

Given the dependence of the HA signal on fixation conditions, our qualitative findings demonstrate that data generated on HA content using the HABP assay cannot be directly compared across different fixatives. Importantly, our study was limited to investigation of fixative-sensitivity of the HABP assay in healthy tissue. Future studies are warranted to examine the effect of fixative condition on HA signal in a pathological setting. Several histochemical studies using the HABP assay have shown that HA abundance and localization is an important feature in several disease processes. For example, one study observed profound changes in HA deposition in inflamed intestinal tissue in an inflammatory bowel disease mouse model, where HA shifted from the epithelial layer to the sub-epithelial layer, and also accumulated in small blood vessels. This was characterized by the authors as a change that would not be reflected in HA content measurements.[35] This observation proved vital for understanding where HA localizes in the early stages of colitis, before immune cell infiltration.[44] Furthermore, HA co-localization with collagen and inflammatory cells provided novel evidence supporting HA's role in organizing an inflammatory response and collagen deposition in antigen-induced pulmonary inflammation.[66] Moreover, our group recently found that Carnoy's fixative is superior to 10% Neutral Buffered Formalin for preserving hepatic HA after carbon tetrachloride-induced liver injury (unpublished observations). Given that different fixation methods can alter our understanding of how HA localization and abundance change through various biological and disease processes, tissue-, and disease-specific HABP staining assay "best practices" are necessary for each organ of

interest and disease process, and with all appropriate negative and positive controls. Establishing a standard of practice will improve the rigor and reproducibility of the HABP assay, which has emerged as an essential tool for the study of HA in situ.

Acknowledgments

We would like to thank Jing Huang for her technical assistance in ovarian tissue sectioning. We also thank board certified pathologists Dr. Tim Fields and Dr. Katie Dennis for their assistance in reviewing and evaluating the kidney and liver histology, respectively. Finally, we would like to acknowledge the late Dr. Mark E. Lauer for the Hyaluronan Binding Protein (HABP) Fluorescent Staining Protocol that he developed as part of the Cleveland Clinic Program of Excellence in Glycoscience—Hyaluronan Matrices in Vascular Pathologies (award number P01HL107147) that was modified for this study.

Competing Interests

The author(s) declared no potential conflicts of interest with respect to the research, authorship, and/or publication of this article.

Author Contributions

MTP and FED designed the experiments. GER, SLM, JER, JS, and NLJ performed the experiments. JER, FED, MTP, and PPK analyzed the data. All authors contributed to manuscript writing and approved the final manuscript.

Funding

The author(s) disclosed receipt of the following financial support for the research, authorship, and/or publication of this article: This work was supported by a Capstone Grant from the Histochemical Society (to GER), R01 HD093726 (to FED and MTP) from the Eunice Kennedy Shriver National Institute of Child Health & Human Development, R01 DK115850 (to PPK) from the National Institute of Diabetes and Digestive and Kidney Diseases, Northwestern University's Center for Reproductive Science Marcia L. Storch Scholarship Fund for Undergraduate Women (to GER), and the Society for Toxicology Summer Undergraduate Research Fellowship (to NLJ). The KUMC Histology Core was supported by the P30 HD002528 (Kansas IDDRC).

Literature Cited

1. Fraser JR, Laurent TC, Laurent UB. Hyaluronan: its nature, distribution, functions and turnover. J Intern Med. 1997;242:27–33.
2. Knudson CB, Knudson W. Cartilage proteoglycans. Semin Cell Dev Biol. 2001;12:69–78.
3. Kultti A, Li X, Jiang P, Thompson CB, Frost GI, Shepard HM. Therapeutic targeting of hyaluronan in the tumor stroma. Cancers (Basel). 2012;4:873–903.
4. Engström PE, Shi XQ, Tronje G, Larsson A, Welander U, Frithiof L, Engstrom GN. The effect of hyaluronan on bone and soft tissue and immune response in wound healing. J Periodontol. 2001;72:1192–200.
5. Cheung WF, Cruz TF, Turley EA. Receptor for hyaluronan-mediated motility (RHAMM), a hyaladherin that regulates cell responses to growth factors. Biochem Soc Trans. 1999;27:135–42.
6. Dowthwaite GP, Edwards JC, Pitsillides AA. An essential role for the interaction between hyaluronan and hyaluronan binding proteins during joint development. J Histochem Cytochem. 1998;46:641–51.
7. Monslow J, Govindaraju P, Pure E. Hyaluronan—a functional and structural sweet spot in the tissue microenvironment. Front Immunol. 2015;6:231.
8. Itano N, Sawai T, Yoshida M, Lenas P, Yamada Y, Imagawa M, Shinomura T, Hamaguchi M, Yoshida Y, Ohnuki Y, Miyauchi S, Spicer AP, McDonald JA, Kimata K. Three isoforms of mammalian hyaluronan synthases have distinct enzymatic properties. J Biol Chem. 1999;274:25085–92.
9. Spicer AP, McDonald JA. Characterization and molecular evolution of a vertebrate hyaluronan synthase gene family. J Biol Chem. 1998;273:1923–32.
10. Csoka AB, Frost GI, Stern R. The six hyaluronidase-like genes in the human and mouse genomes. Matrix Biol. 2001;20:499–508.
11. Monzon ME, Fregien N, Schmid N, Falcon NS, Campos M, Casalino-Matsuda SM, Forteza RM. Reactive oxygen species and hyaluronidase 2 regulate airway epithelial hyaluronan fragmentation. J Biol Chem. 2010;285:26126–34.
12. Soltes L, Mendichi R, Kogan G, Schiller J, Stankovska M, Arnhold J. Degradative action of reactive oxygen species on hyaluronan. Biomacromolecules. 2006;7:659–68.
13. Al'Qteishat A, Gaffney J, Krupinski J, Rubio F, West D, Kumar S, Kumar P, Mitsios N, Slevin M. Changes in hyaluronan production and metabolism following ischaemic stroke in man. Brain. 2006;129:2158–76.
14. Li Y, Rahmanian M, Widstrom C, Lepperdinger G, Frost GI, Heldin P. Irradiation-induced expression of hyaluronan (HA) synthase 2 and hyaluronidase 2 genes in rat lung tissue accompanies active turnover of HA and induction of types I and III collagen gene expression. Am J Respir Cell Mol Biol. 2000;23:411–8.
15. Mack JA, Feldman RJ, Itano N, Kimata K, Lauer M, Hascall VC, Maytin EV. Enhanced inflammation and accelerated wound closure following tetraphorbol ester application or full-thickness wounding in mice lacking hyaluronan synthases Has1 and Has3. J Invest Dermatol. 2012;132:198–207.
16. Tammi R, Pasonen-Seppanen S, Kolehmainen E, Tammi M. Hyaluronan synthase induction and hyaluronan accumulation in mouse epidermis following skin injury. J Invest Dermatol. 2005;124:898–905.
17. Yung S, Thomas GJ, Davies M. Induction of hyaluronan metabolism after mechanical injury of human peritoneal mesothelial cells in vitro. Kidney Int. 2000;58:1953–62.
18. Karousou E, D'Angelo ML, Kouvidi K, Vigetti D, Viola M, Nikitovic D, De Luca G, Passi A. Collagen VI and hyal-

uronan: the common role in breast cancer. Biomed Res Int. 2014;2014:606458.
19. Tammi RH, Kultti A, Kosma VM, Pirinen R, Auvinen P, Tammi MI. Hyaluronan in human tumors: pathobiological and prognostic messages from cell-associated and stromal hyaluronan. Semin Cancer Biol. 2008;18:288–95.
20. Anttila MA, Tammi RH, Tammi MI, Syrjanen KJ, Saarikoski SV, Kosma VM. High levels of stromal hyaluronan predict poor disease outcome in epithelial ovarian cancer. Cancer Res. 2000;60:150–55.
21. Auvinen P, Tammi R, Parkkinen J, Tammi M, Agren U, Johansson R, Hirvikoski P, Eskelinen M, Kosma VM. Hyaluronan in peritumoral stroma and malignant cells associates with breast cancer spreading and predicts survival. Am J Pathol. 2000;156:529–36.
22. Hautmann SH, Lokeshwar VB, Schroeder GL, Civantos F, Duncan RC, Gnann R, Friedrich MG, Soloway MS. Elevated tissue expression of hyaluronic acid and hyaluronidase validates the HA-HAase urine test for bladder cancer. J Urol. 2001;165:2068–74.
23. Lipponen P, Aaltomaa S, Tammi R, Tammi M, Agren U, Kosma VM. High stromal hyaluronan level is associated with poor differentiation and metastasis in prostate cancer. Eur J Cancer. 2001;37:849–56.
24. Pirinen R, Tammi R, Tammi M, Hirvikoski P, Parkkinen JJ, Johansson R, Böhm J, Hollmén S, Kosma VM. Prognostic value of hyaluronan expression in non-small-cell lung cancer: increased stromal expression indicates unfavorable outcome in patients with adenocarcinoma. Int J Cancer. 2001;95:12–7.
25. Sato N, Kohi S, Hirata K, Goggins M. Role of hyaluronan in pancreatic cancer biology and therapy: once again in the spotlight. Cancer Sci. 2016;107:569–75.
26. Schwertfeger KL, Cowman MK, Telmer PG, Turley EA, McCarthy JB. Hyaluronan, inflammation, and breast cancer progression. Front Immunol. 2015;6:236.
27. Bousquet J, Chanez P, Lacoste JY, Enander I, Venge P, Peterson C, Ahlstedt S, Michel FB, Godard P. Indirect evidence of bronchial inflammation assessed by titration of inflammatory mediators in BAL fluid of patients with asthma. J Allergy Clin Immunol. 1991;88:649–60.
28. Roberts CR. Is asthma a fibrotic disease? Chest. 1995;107:111S–7S.
29. Teder P, Vandivier RW, Jiang D, Liang J, Cohn L, Puré E, Henson PM, Noble PW. Resolution of lung inflammation by CD44. Science. 2002;296:155–8.
30. Cowman MK, Lee HG, Schwertfeger KL, McCarthy JB, Turley EA. The content and size of hyaluronan in biological fluids and tissues. Front Immunol. 2015;6:261.
31. Fosang AJ, Hey NJ, Carney SL, Hardingham TE. An ELISA plate-based assay for hyaluronan using biotinylated proteoglycan G1 domain (HA-binding region). Matrix. 1990;10:306–313.
32. Haserodt S, Aytekin M, Dweik RA. A comparison of the sensitivity, specificity, and molecular weight accuracy of three different commercially available Hyaluronan ELISA-like assays. Glycobiology. 2011;21:175–83.
33. Ripellino JA, Klinger MM, Margolis RU, Margolis RK. The hyaluronic acid binding region as a specific probe for the localization of hyaluronic acid in tissue sections: application to chick embryo and rat brain. J Histochem Cytochem. 1985;33:1060–66.
34. Heinegard D, Hascall VC. Aggregation of cartilage proteoglycans. 3. Characteristics of the proteins isolated from trypsin digests of aggregates. J Biol Chem. 1974;249:4250–56.
35. de la Motte CA, Drazba JA. Viewing hyaluronan: imaging contributes to imagining new roles for this amazing matrix polymer. J Histochem Cytochem. 2011;59:252–7.
36. Evanko SP, Potter-Perigo S, Johnson PY, Wight TN. Organization of hyaluronan and versican in the extracellular matrix of human fibroblasts treated with the viral mimetic poly I:C. J Histochem Cytochem. 2009;57:1041–60.
37. McCracken JM, Jiang L, Pritchard MT. Role for a Rhamm-hyaluronan axis in scarless liver repair. Hepatology. 2017;66:207A.
38. Quan N, Harris LR, Halder R, Trinidad CV, Johnson BW, Horton S, Kimler BF, Pritchard MT, Duncan FE. Differential sensitivity of inbred mouse strains to ovarian damage in response to low dose total body irradiation. Biol Reprod. Epub 2019 Aug 22. doi:10.1093/biolre/ioz164
39. Lin W, Shuster S, Maibach HI, Stern R. Patterns of hyaluronan staining are modified by fixation techniques. J Histochem Cytochem. 1997;45:1157–63.
40. Hull RL, Johnson PY, Braun KR, Day AJ, Wight TN. Hyaluronan and hyaluronan binding proteins are normal components of mouse pancreatic islets and are differentially expressed by islet endocrine cell types. J Histochem Cytochem. 2012;60:749–60.
41. Williams SA, Stanley P. Oocyte-specific deletion of complex and hybrid N-glycans leads to defects in preovulatory follicle and cumulus mass development. Reproduction. 2009;137:321–31.
42. Briley SM, Jasti S, McCracken JM, Hornick JE, Fegley B, Pritchard MT, Duncan FE. Reproductive age-associated fibrosis in the stroma of the mammalian ovary. Reproduction. 2016;152:245–60.
43. Latendresse JR, Warbrittion AR, Jonassen H, Creasy DM. Fixation of testes and eyes using a modified Davidson's fluid: comparison with Bouin's fluid and conventional Davidson's fluid. Toxicol Pathol. 2002;30:524–33.
44. Kessler S, Rho H, West G, Fiocchi C, Drazba J, de la Motte C. Hyaluronan (HA) deposition precedes and promotes leukocyte recruitment in intestinal inflammation. Clin Transl Sci. 2008;1:57–61.
45. McCracken JM, Chalise P, Briley SM, Dennis KL, Jiang L, Duncan FE, Pritchard MT. C57BL/6 substrains exhibit different responses to acute carbon tetrachloride exposure: implications for work involving transgenic mice. Gene Expr. 2017;17:187–205.
46. McCracken JM, Jiang L, Deshpande KT, O'Neil MF, Pritchard MT. Differential effects of hyaluronan synthase 3 deficiency after acute vs chronic liver injury in mice. Fibrogenesis Tissue Repair. 2016;9:4.
47. Fischer AH, Jacobson KA, Rose J, Zeller R. Hematoxylin and eosin staining of tissue and cell sections CSH Protoc. 2008;2008:prot4986.

48. Magoffin DA. Ovarian theca cell. Int J Biochem Cell Biol. 2005;37:1344–9.
49. Suchanek E, Simunic V, Juretic D, Grizelj V. Follicular fluid contents of hyaluronic acid, follicle-stimulating hormone and steroids relative to the success of in vitro fertilization of human oocytes. Fertil Steril. 1994;62:347–52.
50. Hansell P, Goransson V, Odlind C, Gerdin B, Hallgren R. Hyaluronan content in the kidney in different states of body hydration. Kidney Int. 2000;58:2061–8.
51. Bancroft JD. Theory and practice of histological techniques. 6th ed. Philadelphia: Churchill Livingstone/Elsevier; 2008.
52. Rolls G. Fixation and fixatives: Popular fixative solutions. Wetzlar: Leica Biosystems; 2012.
53. Chung JY, Song JS, Ylaya K, Sears JD, Choi L, Cho H, Rosenberg AZ, Hewitt SM. Histomorphological and molecular assessments of the fixation times comparing formalin and ethanol-based fixatives. J Histochem Cytochem. 2018;66:121–35.
54. Salustri A, Camaioni A, Di Giacomo M, Fulop C, Hascall VC. Hyaluronan and proteoglycans in ovarian follicles. Hum Reprod Update. 1999;5:293–301.
55. Camenisch TD, Spicer AP, Brehm-Gibson T, Biesterfeldt J, Augustine ML, Calabro A, Kubalak S, Klewer SE, McDonald JA. Disruption of hyaluronan synthase-2 abrogates normal cardiac morphogenesis and hyaluronan-mediated transformation of epithelium to mesenchyme. J Clin Invest. 2000;106:349–60.
56. Stridh S, Kerjaschki D, Chen Y, Rugheimer L, Astrand AB, Johnsson C, Friberg P, Olerud J, Palm F, Takahashi T, Ikegami-Kawai M, Hansell P. Angiotensin converting enzyme inhibition blocks interstitial hyaluronan dissipation in the neonatal rat kidney via hyaluronan synthase 2 and hyaluronidase 1. Matrix Biol. 2011;30:62–9.
57. Goransson V, Johnsson C, Jacobson A, Heldin P, Hallgren R, Hansell P. Renal hyaluronan accumulation and hyaluronan synthase expression after ischaemia-reperfusion injury in the rat. Nephrol Dial Transplant. 2004;19:823–30.
58. Stridh S, Palm F, Hansell P. Renal interstitial hyaluronan: functional aspects during normal and pathological conditions. Am J Physiol Regul Integr Comp Physiol. 2012;302:R1235–49.
59. Armstrong SE, Bell DR. Measurement of high-molecular-weight hyaluronan in solid tissue using agarose gel electrophoresis. Anal Biochem. 2002;308:255–64.
60. Nanji AA, Tahan SR, Khwaja S, Yacoub LK, Sadrzadeh SM. Elevated plasma levels of hyaluronic acid indicate endothelial cell dysfunction in the initial stages of alcoholic liver disease in the rat. J Hepatol. 1996;24:368–74.
61. Stickel F, Poeschl G, Schuppan D, Conradt C, Strenge-Hesse A, Fuchs FS, Hofmann WJ, Seitz HK. Serum hyaluronate correlates with histological progression in alcoholic liver disease. Eur J Gastroenterol Hepatol. 2003;15:945–50.
62. Tsutsumi M, Urashima S, Takase S, Ueshima Y, Tsuchishima M, Shimanaka K, Kawahara H. Characteristics of serum hyaluronate concentrations in patients with alcoholic liver disease. Alcohol Clin Exp Res. 1997;21:1716–21.
63. Yagmur E, Koch A, Haumann M, Kramann R, Trautwein C, Tacke F. Hyaluronan serum concentrations are elevated in critically ill patients and associated with disease severity. Clin Biochem. 2012;45:82–7.
64. Yagmur E, Tacke F, Weiss C, Lahme B, Manns MP, Kiefer P, Trautwein C, Gressner AM. Elevation of Nepsilon-(carboxymethyl)lysine-modified advanced glycation end products in chronic liver disease is an indicator of liver cirrhosis. Clin Biochem. 2006;39:39–45.
65. Urashima S, Tsutsumi M, Shimanaka K, Ueshima Y, Tsuchishima M, Itoh T, Kawahara H, Takase S. Histochemical study of hyaluronate in alcoholic liver disease. Alcohol Clin Exp Res. 1999;23:56S–60S.
66. Cheng G, Swaidani S, Sharma M, Lauer ME, Hascall VC, Aronica MA. Hyaluronan deposition and correlation with inflammation in a murine ovalbumin model of asthma. Matrix Biol. 2011;30:126–34.